Jet Charge Method for c/$\bar{c}$ Tagging

Shalhout Zaki Shalhout

Physics Department, Wayne State University, Detroit, MI, 48201

Abstract

In this study jet charge is examined as a potential tag for c and $\bar{c}$. Jet charges are calculated for both simulated and actual events containing D^0 or $\bar{D}^0$ mesons that have a $D^{*\mp}$ as their parent particle. The resulting jet charge distributions for D^0 and $\bar{D}^0$ jets differ, suggesting that the jet charge can be used to tag c and $\bar{c}$.

Introduction

Since color neutrality must be maintained for all systems, when a c or $\bar{c}$ is created by an e^+ e^- collision, additional quarks appear from the vacuum in the right combination to maintain the colorless status of the event. The particles formed from these additional quarks make up the charm jet.

The different charges of the c quark and $\bar{c}$ quark (+ 2/3 and -2/3 respectively) suggest the charges of the additional quarks and the particles formed from them will differ between the c and $\bar{c}$ cases. This 'jet charge' has the potential to serve as a c and $\bar{c}$ tag.

In this study the jet charge is calculated for both simulated and real events containing a D^0 and/or a $\bar{D}^0$. Since the D^0 is composed of a c and $\bar{u}$, the events containing a D^0 are used to calculate a c jet charge. Likewise, the $\bar{D}^0$ is composed of a $\bar{c}$ and u therefore; the events containing a $\bar{D}^0$ are used to calculate a $\bar{c}$ jet charge. Figure 1 is a diagram of the fragmentation of the c and $\bar{c}$ quarks showing the additional charge. Once this additional charge is used to calculate the jet chrges for a number of events, the distributions of c jet charge and the distributions of $\bar{c}$ jet charge are then compared.

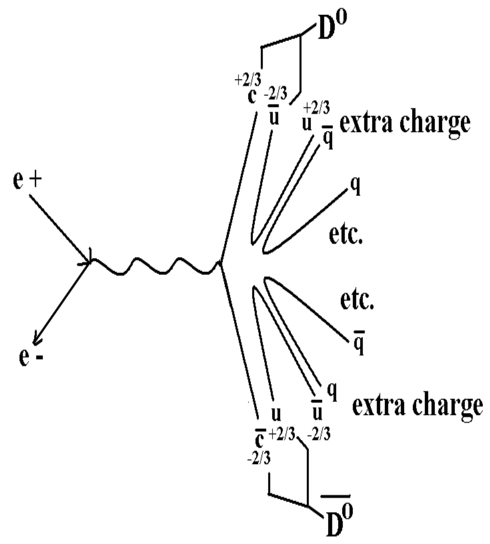

FIGURE 1. A diagram of the fragmentation of the c and $\bar{c}$ quarks showing the additional charge.

The method used in the calculation of jet charges is drawn from the techniques used by the ALEPH collaboration [1] in measuring the jet charge in Z decays, and [2] in measuring charge asymmetry in hadronic Z decays.

Method of Jet Charge Calculation

In order to calculate the jet charge of an event, the event must be assigned a jet axis. Here the jet charge was calculated twice for each event. First the jet charge was calculated using the momentum of the D^0 or the $\bar{D}^0$ as the jet axis. Then it was recalculated using the thrust vector of the event as the jet axis, using the equation

$$\sum_{i=1}^{n} |\vec{N_{thrust}} \cdot \vec{p_i}| = maximum \tag{1}$$

where n is the number of particles in the event, $\vec{p_i}$ is the momentum of each particle, and $\vec{N}_{\mathrm{thrust}}$ is the thrust vector which maximizes the sum.

Both methods of assigning jet axis have their advantages. The use of the D^0 or $\bar{D}^0$ momentum has the advantage of defining the axis along the direction of travel of the particle containing the c or $\bar{c}$ quark. This gives a greater weight to the charges of particles closest to the c or $\bar{c}$ in the jet charge calculation. The main advantage of using thrust as the axis is that the calculation of thrust does not require the presence of a reconstructed D^0 or $\bar{D}^0$ in the event, as does the use of momentum. The jet charge distributions obtained using these two methods are compared below.

Once the jet axis has been defined, the event must be divided into two hemispheres, front and back. By convention, the front hemisphere is always the hemisphere towards which the thrust axis points. The other hemisphere is the back hemisphere.

The jet charge is calculated as the sum of the charges of the charged tracks in a given hemisphere, with the charges weighted by their momentums with respect to the jet axis (thrust or $D^0/\bar{D}^0$ momentum) of the event.

The formulas used to calculate jet charge are

$$jet\ charge\ _{front} = \frac{\sum^{\vec{p_i}\cdot\vec{a}>0}\ q_i * |\vec{a}\cdot\vec{p_i}|^{\kappa}}{\sum^{\vec{p_i}\cdot\vec{a}>0}\ |\vec{a}\cdot\vec{p_i}|^{\kappa}} \tag{2}$$

and

$$jet\ charge\ _{back} = \frac{\sum^{\vec{p_i}\cdot\vec{a}<0}\ q_i * |\vec{a}\cdot\vec{p_i}|^{\kappa}}{\sum^{\vec{p_i}\cdot\vec{a}<0}\ |\vec{a}\cdot\vec{p_i}|^{\kappa}} \tag{3}$$

where, $\vec{p_i}$ is the momentum of a track in the event, $\vec{a}$ is the jet axis (thrust or $D^0/\bar{D}^0$ momentum) of the event, q_i is the charge of a particle, and the parameter κ is a weighting factor whose value dictates the degree to which the particles' charges are actually weighted by their momentums. Its value was adjusted to give the maximum separation between c and $\bar{c}$ jet charge distributions.

Equation 2 is used to calculate jet charge in the front hemisphere, while Equation 3 is used to calculated jet charge in the back hemisphere. In Equation 2 the sum is taken over particles for which $\vec{p_i} \cdot \vec{a} > 0$, and in Equation 3 the sum is taken over particles for which $\vec{p_i} \cdot \vec{a} < 0$.

When the momentum of a D^0 or a $\bar{D}^0$ is used as the jet axis, the location of the D^0 or the $\bar{D}^0$ in the event is used to determine weather Equation 2 or Equation 3 is used. If the D^0 or $\bar{D}^0$ is in the front hemisphere (that is $\vec{N}_{thrust} \cdot \vec{p}_{D^0 or \bar{D}^0} > 0$) then Equation 2 is used. If the D^0 or $\bar{D}^0$ is in the back hemisphere of the event (that is $\vec{N}_{thrust} \cdot \vec{p}_{D^0 or \bar{D}^0} < 0$) then Equation 3 is used in the calculation of jet charge.

Determination of the value of κ

In order to determine the value of κ that maximizes the differences between two distributions, some parameter must be defined which quantifies the amount of difference present. The chosen parameter is called 'separation' and is defined as,

$$\sum_{i=1}^{b} [F_i^c - F_i^{\bar{c}}]^2 = separation \tag{4}$$

where b is the number of bins on a histogram, where F_i^c is the fraction of c tags that fall in a given bin and $F_i^{\bar{c}}$ is the fraction of $\bar{c}$ tags in the same bin.

Two populations of particles were used in the determination of the appropriate value of κ. The first population consisted exclusively of D^0's and $\bar{D}^0$'s which came directly from an $e^+ e^-$ collision. The particles in this population had no intermediate parent particles, instead coming directly from a virtual photon (vpho). The second population consisted exclusively of D^0's and $\bar{D}^0$'s that did not come directly from an $e^+ e^-$ collision (non-vpho).

Separation values over a range of κ values were calculated two times for each of the two populations. First using thrust, and second using momentum as the jet axis. In addition, both of these calculations were done for two types of simulated events, QQ and Cleog/Pass2 Monte Carlo. The results are shown in plots of separation verses κ. These can be seen in Figure 2.

FIGURE 2. Plots of separation vs. κ for QQ and Cleog/Pass2 Monte Carlo data.

For each case the value of separation approaches infinity as κ increases and negative infinity as κ decreases. Despite the greater separations the jet charge distributions obtained for large κ provided little useful information as the distributions are distorted by a larger tendency for the jet charge to equal 1 or -1. In addition each plot shows a local maximum in the value of separation when κ is equal to negative one half. Since the jet charge distributions here are less biased by occurrences of 1 and -1, the value of κ is chosen to be negative one half.

Jet Charge Distributions for Simulated Events

After fixing the value of κ at negative one half, jet charge distributions were obtained for 58,000 QQ simulated events and 58,000 Cleog/Pass2 Monte Carlo simulated events. Both groups were made up of simulated events containing a D^0 and/or a $\bar{D}^0$.

Theses distributions were plotted primarily to verify whether or not any differences between the c and $\overline{c}$ cases would exist. A few representative distributions can be seen in Figure 3. The plots show the jet charge distributions obtained from QQ data in red and with the secondary identification number (IDB) equal to one. The jet charge distributions obtained from Cleog/Pass2 Monte Carlo data are shown in green and have a secondary identification number (IDB) equal to two.

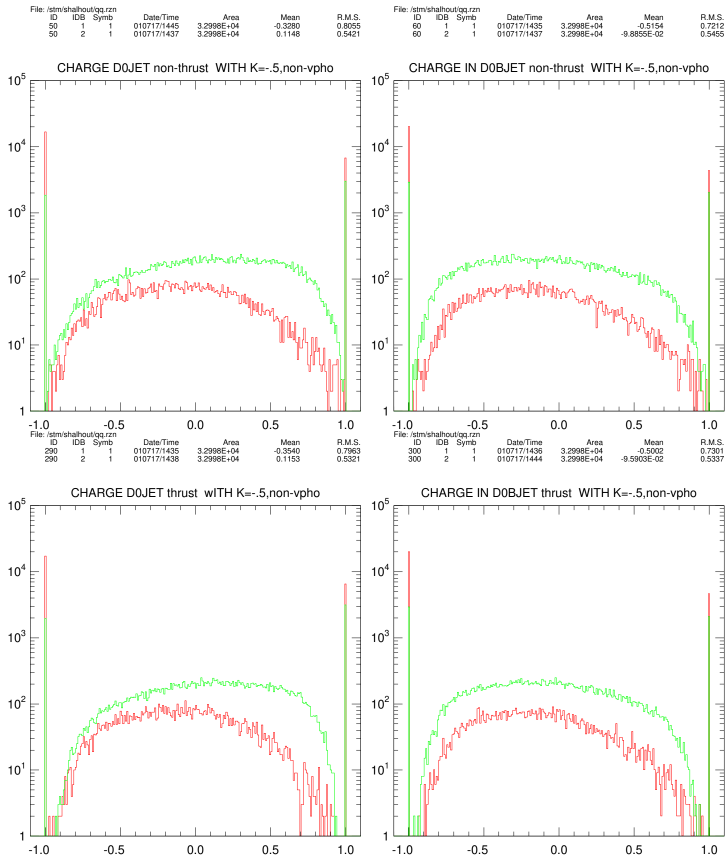

FIGURE 3. Histograms showing the jet charge distribution obtained from QQ data in red, with the secondary identification number (IDB) equal to one. The jet charge distribution obtained from Cleog/Pass2 Monte Carlo data is shown in green and has a secondary identification number (IDB) equal to two.

The distributions obtained for the QQ data differ somewhat from the distributions obtained for the Cleog/Pass2 Monte Carlo in overall shape and mean jet charge value. These differences are not unexpected since the two simulation types differ dramatically in the degree to which they approximate reality.

A more useful comparison can be made between the c (D^O) and $\bar{c}$ ($\bar{D^O}$) jet charge distributions obtained for each data type. The differences between QQ and Cleog/Pass2 Monte Carlo mean c jet charge and QQ and Cleog/Pass2 Monte Carlo mean $\bar{c}$ jet charge are compared in table 1 below.

TABLE 1. Differences in mean c and $\bar{c}$ jet charge for QQ and Pass2/Cleog simulated events

Axis Method/VPHO or non-VPHO	QQ mean difference	Pass2/Cleog mean difference
Thrust/ VPHO	.1797	.2209
Thrust/ non-VPHO	.1462	.2112
momentum/ VPHO	.2332	.2395
momentum/non-VPHO	.1874	.2133

Table one displays the differences between the mean values of the jet charge distributions for the D^0 and $\bar{D}^0$ cases. The jet charge distributions were calculated using the same two particle populations used in the determination of the value of κ. That is, one population consisting of D^0's and $\bar{D}^0$'s which came directly from an e^+ e^- collision (vpho) and one population consisting exclusively of D^0's and $\bar{D}^0$'s that did not come directly from an e^+ e^- collision (non-vpho). As in the determination of the value of κ, the jet charge distributions were obtained twice, once using thrust as the jet axis (thrust), and once using the momentum of the D^0 or $\bar{D}^0$ as the jet axis (non-thrust). In addition, since the identity of the D^0 or $\bar{D}^0$ in each simulated event was known, separate jet charge distributions were obtained for c and $\overline{c}$ jets.

The fact that the difference between the mean D^0 jet charge and the mean $\bar{D}^0$ jet charge is non-zero for all QQ and Cleog/Pass2 Monte Carlo distributions, confirms that the c and $\overline{c}$ jet charge distributions are not the same. That implies that the jet charge can be used as a tag for c and $\overline{c}$.

Comparison of Jet Charge Distribution for Real and Simulated Events

The c and $\overline{c}$ jet charge distributions obtained from an analysis of one million hadron skim events, were compared to the c and $\overline{c}$ jet charge distributions obtained by running the same analysis on one-hundred thousand Cleog/Pass2 Monte Carlo simulated events, each of which was known to contain a D^0 and/or a $\bar{D}^0$.

To obtain accurate jet charge distributions for non-simulated c and $\overline{c}$ events, a pure population of D^0's and $\bar{D}^0$'s was isolated. To further minimize background, the population was limited by the exclusion of all but one type of D^0; those created in the decay process

$$D^{*-} \rightarrow \pi_2^- D^0 \rightarrow K^- \pi_1^+ \tag{5}$$

were selected. Likewise, only one type of $\bar{D}^0$ was included in the population; those created in the decay process

$$D^{*+} \rightarrow \pi_2^+ D^0 \rightarrow K^+ \pi_1^- \tag{6}$$

These same populations were then isolated from the Cleog/Pass2 Monte Carlo. This was done in order to allow comparisons of jet charge distributions for events containing members of these populations.

To select events that would contain particles belonging to one of the two populations, the following analysis was conducted for each event. First, each track in an event that had a charge of absolute value equal to one was assigned the mass of the $K^{\mp}$ particle. Then every other track that had a charge of absolute value also equal to one, was assigned the mass of the $\pi^{\mp}$. Next, each track that was assigned the $\pi^{\mp}$ mass was matched to each track that had been assigned the mass of the $K^{\mp}$. If the product of the charges of the two tracks was equal to negative one (that is if they were K^- and π^+ or K^+ and π^-), their invariant masses were calculated using the formula

$$mass\,of\;D^0\;or\;\bar{D}^0 = \sqrt{(E_{K^{\mp}} + E_{\pi_1^{\mp}})^2 - (\vec{P_{K^{\mp}}} + \vec{P_{\pi_1^{\mp}}}) * (\vec{P_{K^{\mp}}} + \vec{P_{\pi_1^{\mp}}})} \tag{7}$$

where, $E_{K^{\mp}}$ is the energy of the $K^{\mp}$,$E_{\pi_1^{\mp}}$ is the energy of the $\pi_1^{\mp}$, $\vec{P_{K^{\mp}}}$ is the momentum of the $K^{\mp}$, and $\vec{P_{\pi_1^{\mp}}}$ is the momentum of the $\pi_1^{\mp}$.

The resulting invariant mass distributions are shown in Figure 4. The distributions were fit using a second order polynomial function and a Gaussian function. The portion of each distribution falling under the Gaussian fit was taken to represent the distribution of D^0 and $\bar{D}^0$ invariant masses.

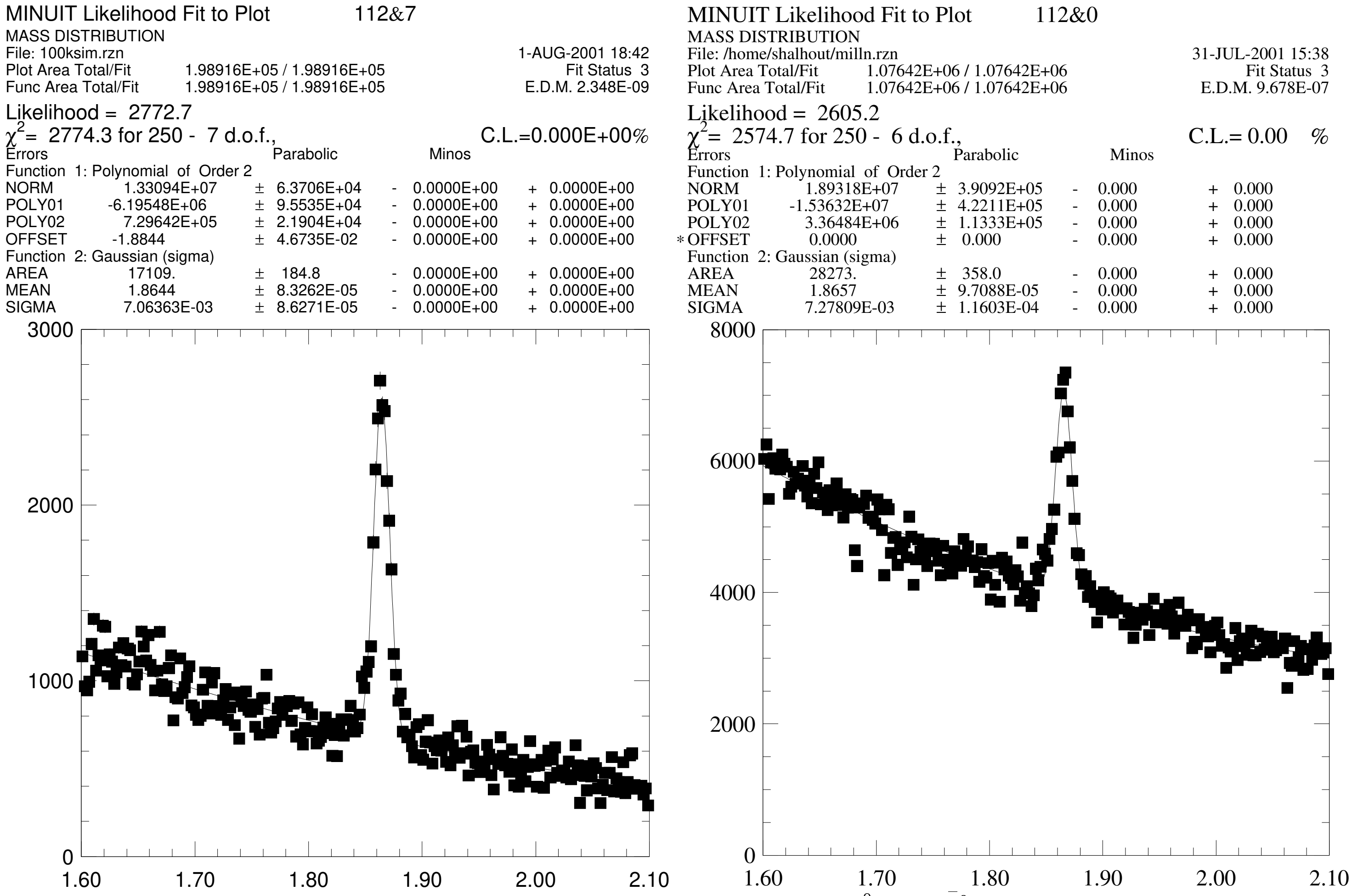

FIGURE 4. Histograms showing the distribution of likley D^0 and $\bar{D}^0$ masses. The distribution on the left was obtained from simulated events, while the distribution on the right was obtained from real events.

From this distribution a range for D^0 and $\bar{D}^0$ invariant masses was chosen as

$$mass\ range = Gaussian\ mean \mp 3 * \sigma \tag{8}$$

where σ is the Gaussian standard deviation. Table 2 shows the calculated ranges.

TABLE 2. calculated ranges for D^0 and $\bar{D}^0$ invariant masses (GeV)

Data Type	mean	Range
Cleog/Pass2 Monte Carlo simulated	1.8644	1.8644∓.02119
Real Data	1.8657	1.8657∓.02183

Once this range was calculated for both the real and the simulated event sets, it was used to identify events that did not have a combination of two tracks that could have come from a D^0 or a $\bar{D}^0$ Jet charges were not calculated for these events, leaving only events containing a potential D^0 or $\bar{D}^0$ to contribute to the jet charge distributions.

For events that had a potential D^0 or $\bar{D}^0$ with an invariant mass in the above range, each track with a charge of one or negative one except the two that had been previously assigned a mass were assigned the mass of a $\pi^{\mp}$. If the three tracks assigned masses of $K^{\mp}$,$\pi^{\mp}$, and $\pi^{\mp}$, had charges of -1, +1, -1 or +1, -1, +1 respectively, then an invariant mass for the $D^{*\mp}$ was calculated with the equation

$$D^{*\mp}\,mass = \sqrt{(E_{K^{\mp}} + E_{\pi_1^{\mp}} + E_{\pi_2^{\mp}})^2 - (\vec{P_{K^{\mp}}} + \vec{P_{\pi_1^{\mp}}} + \vec{P_{\pi_2^{\mp}}}) * (\vec{P_{K^{\mp}}} + \vec{P_{\pi_1^{\mp}}} + \vec{P_{\pi_2^{\mp}}})} \tag{9}$$

where, $E_{K^{\mp}}$ is the energy of the $K^{\mp}$,$E_{\pi_1^{\mp}}$ is the energy of the $\pi_1^{\mp}$,$E_{\pi_2^{\mp}}$ is the energy of the $\pi_2^{\mp}$, $\vec{P_{K^{\mp}}}$ is the momentum of the $K^{\mp}$, $\vec{P_{\pi_1^{\mp}}}$ is the momentum of the $\pi_1^{\mp}$, and $\vec{P_{\pi_2^{\mp}}}$ is the momentum of the $\pi_2^{\mp}$.

Next a Q value was calculated using the equation

$$Q = D^{*\mp}_{mass} - D^{0\mp}_{mass} - \pi^{\mp}_{2\,mass} \tag{10}$$

The Q value distributions for each type of data were plotted in histograms and can be seen in Figure 5. The Q value distributions were fit using threshold and Gaussian functions.

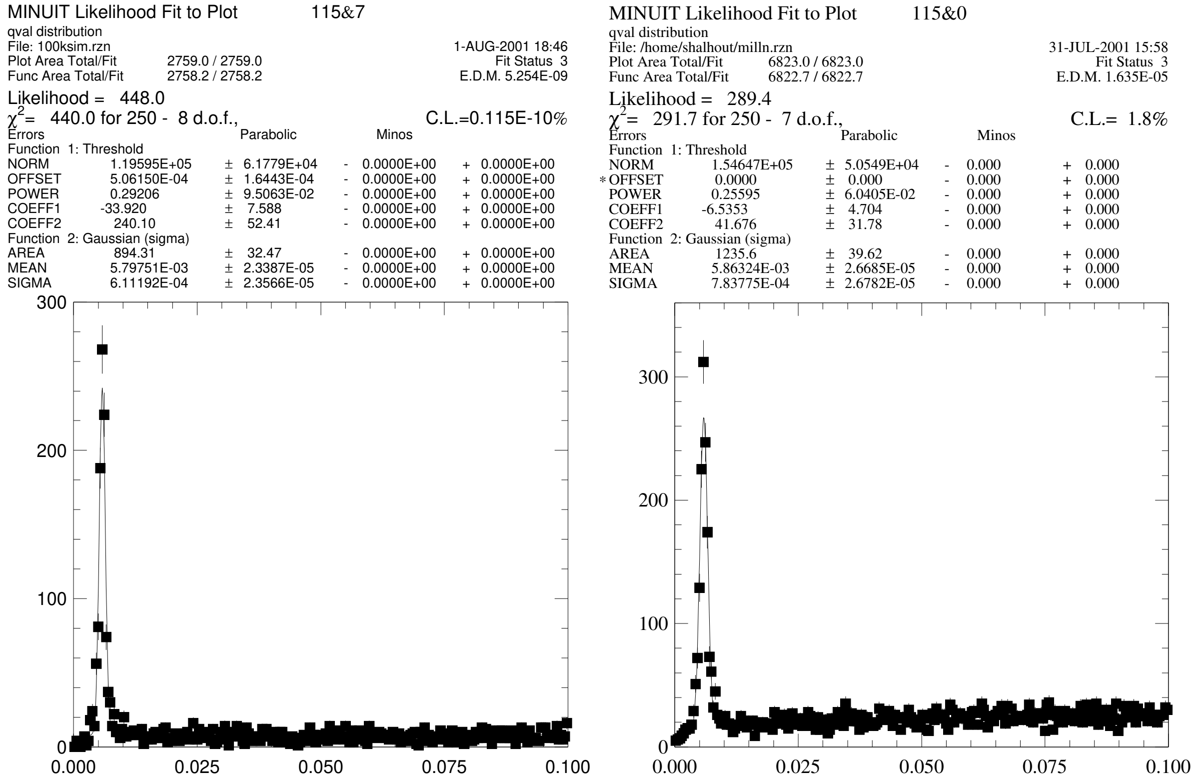

FIGURE 5. Histograms showing the distribution of Q values. The distribution on the left was obtained from simulated events, while the distribution on the right was obtained from real events.

The mean and sigma of the Gaussian region of the distribution were used to calculate the range

$$Q\ range = Gaussian\ mean \mp 3 * \sigma \tag{11}$$

where σ is the Gaussian standard deviation. Table 3 shows the calculated ranges.

TABLE 3. calculated ranges for Q values (GeV)

Data Type	mean	Range
Cleog/Pass2 Monte Carlo simulated	5.79751e-3	5.79751e-3∓1.8335e-3
Real Data	5.86324e-3	5.86324e-3∓2.35132e-3

Those events that had Q values in the above ranges of the distribution, were taken to be events that had a D^0 that came from the decay of a D^{*-}, and/or events that had a $\bar{D}^0$ that came from the decay of a D^{*+}. Jet charges were only calculated for these events, excluding all events that did not contain a D^0 or a $\bar{D}^0$ from the two populations discussed above.

The charge of the track assigned the mass of the $K^{\mp}$ was used to identify each non-excluded event as containing either a D^0 or a $\bar{D}^0$. If the charge of this track was negative one, then the event contained a D^0 and its jet charge was included in the c jet charge distribution. If the charge of this track was positive one, then the event contained a D^0 and its jet charge was included in the $\bar{c}$ jet charge distribution.

The jet charge distributions obtained for the events with D^0 and/or $\bar{D}^0$ invariant masses and Q values falling within the ranges shown in Tables 2 and 3 are shown in Figure 6. In these figures the distributions obtained from simulated data are plotted over the distributions obtained from real data. The simulated distributions are in blue and have a secondary identification number (IDB) equal to 7. The real distributions are in red and have a secondary identification number (IDB) equal to 0.

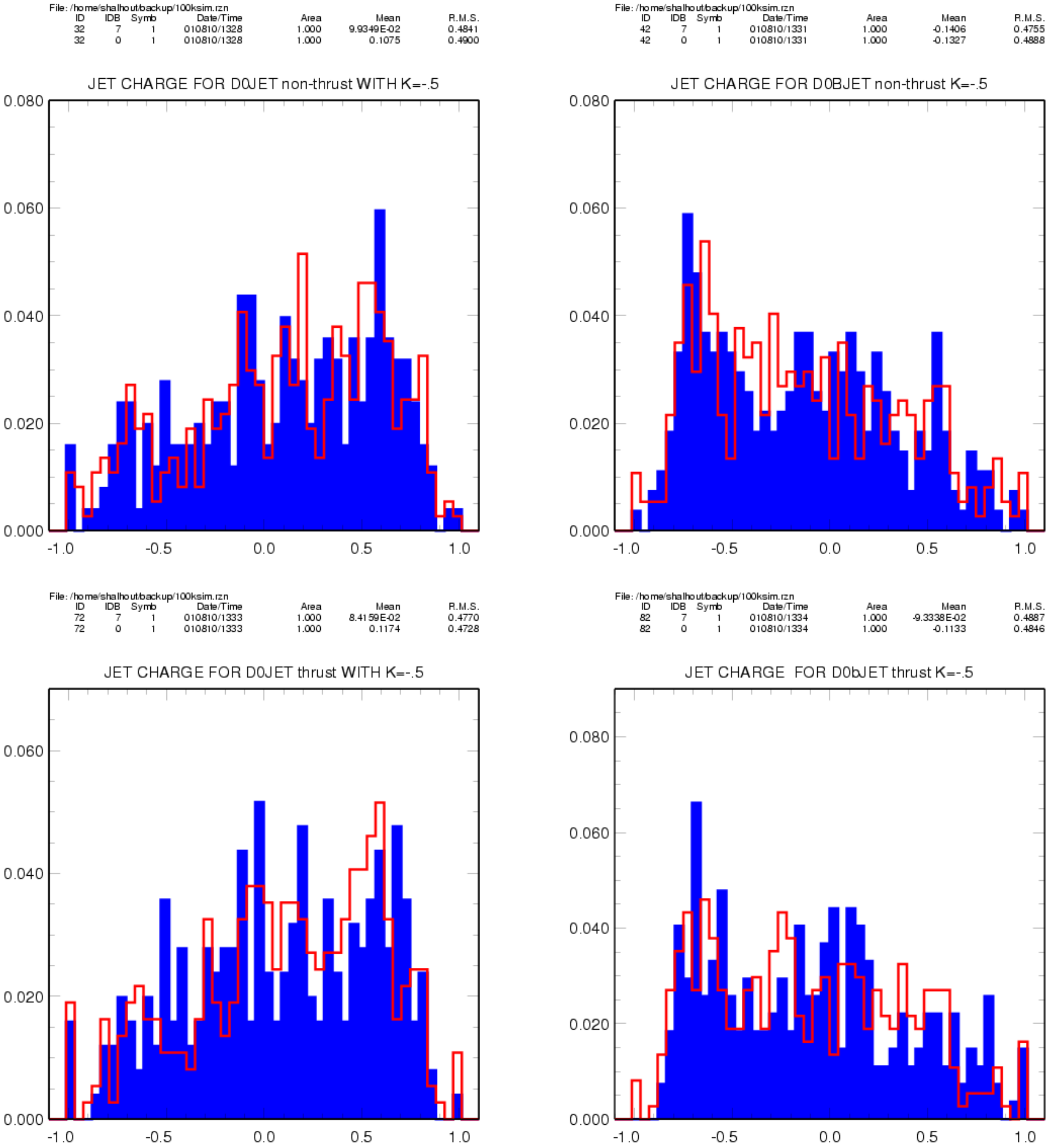

FIGURE 6. Comparison between jet charge distributions obtained from real and simulated data (approximatly 1000 events per data type). The simulated distributions are in blue and have secondary identification numbers (IDB) equal to 7. The real distributions are in red and have secondary identification numbers (IDB) equal to 0.

The distributions obtained from both simulated and real data agree on the general shape of the c (D^0) and $\bar{c}$ ($\bar{D^0}$) distributions; both suggest that a c jet charge is more likely to be positive, while an $\bar{c}$ jet charge is more likely to be negative. These conclusions are supported by comparisons of mean jet charges made in Table 4.

TABLE 4. Comparison of Simulated and Real mean jet charges

c or $\bar{c}$ jet	thrust or momentum	real mean jet charge	simulated mean jet charge	% difference
c	momentum	.1067	9.9384e-3	7.1
$\bar{c}$	momentum	-.1329	-.1421	6.69
c	thrust	.1167	8.3600e-2	33.1
$\bar{c}$	thrust	-.1126	-9.3468e-2	18.6

According to Table 4, the jet charge distributions obtained from both real and simulated data agree that the mean jet charge should be negative for $\bar{c}$ jets and positive for c jets. However, the larger percent differences between real and simulated mean jet charges when using thrust as the jet axis, suggest that the simulated jet charge distributions are closer to reality when momentum is used instead.

Figure 7 shows overlapping comparisons of c and $\bar{c}$ jet charge distributions. The c jet charge distributions are in black while the $\bar{c}$ jet charge distributions are in green. The $\bar{c}$ distributions have the greater identification number (ID) in each case. Simulated distributions have a secondary identification number (IDB) equal to 7, while real distributions have a secondary identification number (IDB) equal to 0.

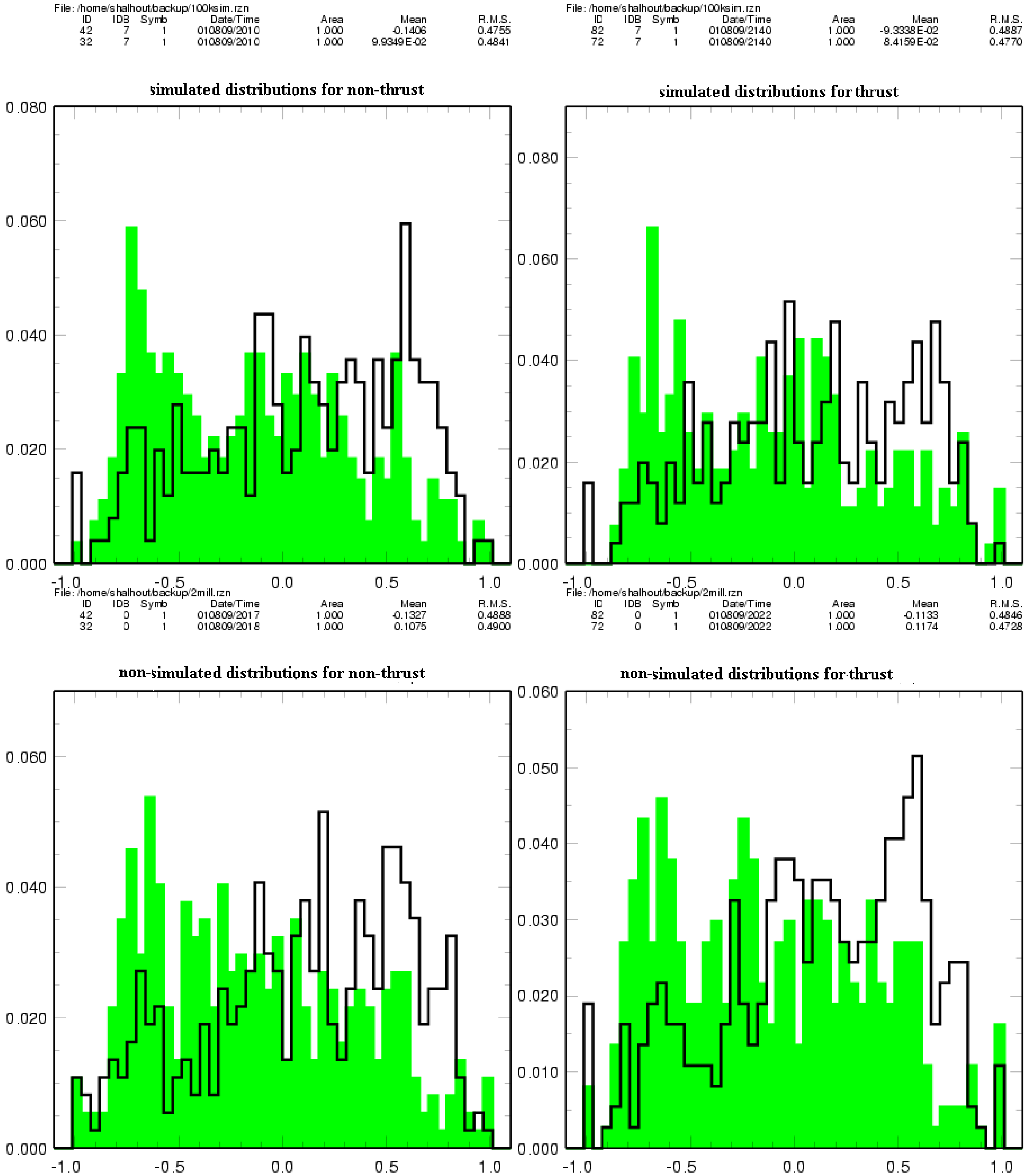

FIGURE 7. Overlapping comparisons of c and $\bar{c}$ jet charge distributions. The c jet charge distributions are in black while the $\bar{c}$ jet charge distributions are in green. Simulated distributions have a secondary identification number (IDB) equal to 7, while real distributions have a secondary identification number (IDB) equal to 0.

Table 5 lists the mean jet charge and the separation between the distributions for the c and $\bar{c}$ cases.

TABLE 5. Comparison of c and $\bar{c}$ jet charge distributions

thrust/momentum	data type	c mean	$\bar{c}$ mean	separation
momentum	simulated	9.9384e-2	-.1421	103.20
thrust	simulated	8.3600e-2	-9.3468e-2	95.44
momentum	real	.1067	-.1329	97.40
thrust	real	.1167	-.1126	82.77

Table 5 shows that the separations between c jet charge distributions and $\bar{c}$ jet charge distributions are large. Since the separations are large and the overall means are different for c and $\bar{c}$ jet charges, jet charge has the potential to serve as a c and c-bar tag.

Results

The plots in Figure 7 above show that the jet charge distributions obtained for c and $\bar{c}$ jets are different. According to the results obtained using simulated events the mean of the c jet charge distribution should be positive, while the mean of the $\bar{c}$ jet charge distribution should be negative.

This agrees with the results obtained from non-simulated events where the c jet charge distribution has means of .1067 (with momentum of $D^0/\bar{D}^0$ as jet axis) and .1167 (with thrust as jet axis), while the $\bar{c}$ jet charge distribution has means of -.1329 (with momentum of $D^0/\bar{D}^0$ as jet axis) and -.1126(with thrust as jet axis).

Although the difference in the c and $\bar{c}$ jet charge distributions implies that the jet charge can in fact be used as a c and $\bar{c}$ tag, distributions must be obtained for a much larger number of events before more concrete conclusions can be drawn.

Conclusions and Future Work

This study has shown that jet charge distributions are not the same for c and $\bar{c}$ jets. This difference was found in both simulated and real events, and suggests that jet charge can distinguish between c and $\bar{c}$. In order to confirm these preliminary results, jet charge distributions must be obtained for a larger number of events, and those distributions must be analyzed more closely. Future work will also include a search for wrong sign decays of the D^0 and $\bar{D}^0$.

Acknowledgments

I am pleased to acknowledge Professor Dave Cinabro, of Wayne State University, who proposed this Research Experience for Undergraduates project and guided my efforts throught the summer. I would also like to thank Gradstudent Sean McGee and Postdoc Mikhail Dubrovin, both of Wayne State University for a great deal of advice and assistance on this project. I would also like to thank the REU directors at Cornell Universtity, and the Wayne State faculty who helped to prepare me for this experience. This work was supported by National Science Foundation REU grants NSF-PHY-0113556 and PHY-0097595 and research grant PHY-9809799.

References

1. ALEPH Collaboration, Phys. Lett. B 426 (1998) 217.
2. ALEPH Collaboration, Phys. Lett. B 259 (1991) 357.